Hindawi
Journal of Sensors
Volume 2018, Article ID 4176314, 12 pages
https://doi.org/10.1155/2018/4176314

Research Article

Power Transmission Tower Monitoring with Hydrostatic Leveling System: Measurement Refinement and Performance Evaluation

Xingfu Zhang,[1] Yongyi Zhang,[2] Lei Zhang,[3] Guangxin Qiu,[2] and Dehong Wei[1]

[1]*Department of Surveying Engineering, Guangdong University of Technology, Guangzhou 510006, China*
[2]*Guangzhou Urban Planning & Design Survey Research Institute, Guangzhou 510000, China*
[3]*Department of Land Surveying and Geo-Informatics, The Hong Kong Polytechnic University, Hong Kong*

Correspondence should be addressed to Lei Zhang; lslzhang@polyu.edu.hk

Received 19 April 2018; Revised 15 August 2018; Accepted 26 September 2018; Published 30 December 2018

Academic Editor: Romeo Bernini

A hydrostatic leveling system (HLS) is an automated high-accuracy measurement technology widely used for vertical displacement monitoring. This paper focuses on evaluating the performance of HLS for monitoring the deformation of a power transmission tower base together with a slope sensor and displacement meter. The monitoring results show that HLS measurements are strongly affected by the environmental temperature. Therefore, to obtain the actual deformation of a monitoring target, the measurements should be further processed to reduce the effect of temperature on the result. To this end, four data processing schemes are proposed, which are based on the frequency of processing (i.e., day by day, monthly, quarterly, or annually). The results demonstrate that the quarterly processing scheme effectively reduces the impact of temperature on deformation measurements and therefore provides the most accurate results among the four schemes considered. Since after correction, the HLS measurements are consistent with the independent monitoring results obtained from the slope sensor and displacement meter, the proposed correction strategy is workable and might be considered for similar monitoring scenarios in future.

1. Introduction

Vertical displacement monitoring is important for evaluating the health status of infrastructures. Numerous methods of vertical displacement monitoring have been employed, such as precise leveling, trigonometric leveling, global navigation satellite system (GNSS) technology, and hydrostatic leveling systems (HLSs). Among these methods, HLS is a highly accurate, automated, and widely used measurement technology. The measurement accuracy of an HLS is around mm level and can even approach up to 1 μm [1]. Due to the high degree of automation and continuous operation with high measurement accuracy, HLSs have been widely applied in difficult circumstances such as conditions involving high radiation, high risk, limited space, and air turbulence. For example, successful monitoring of bridge variations with HLSs have been reported in [2–6], and the measurement results obtained showed a satisfied agreement with the results of strain and stress measurements. Moreover, continuous long-term monitoring results obtained from HLS have provided essential information for deformation modeling and for guaranteeing the structural safety of bridges. Yin [7] applied the HLS to measure the vertical displacement responses of metropolitan train tunnels; the capacity for automation and continuity of the method provided a definite advantage over precise leveling which cannot be employed for monitoring during the train operation period. Martin [8] applied an HLS composed of more than 500 sensors to measure the vertical displacement responses of the European Synchrotron Radiation Facility (ESRF), and the system demonstrated a precision of about 1 to 3 μm over short periods, which has a satisfied agreement with level and tilt survey data. In particular, the HLS has also been successfully employed to control the vertical movements induced by jacks during machine realignment. For example, Wei et al. [9] applied an HLS composed of 192 sensors to monitor the vertical position as well as the pitch and yaw of the magnet girders in the Swiss Light Source (SLS) storage ring and obtained a micrometer-range precision over short periods. An experience of three years with the HLS employed in the SLS storage ring revealed not only

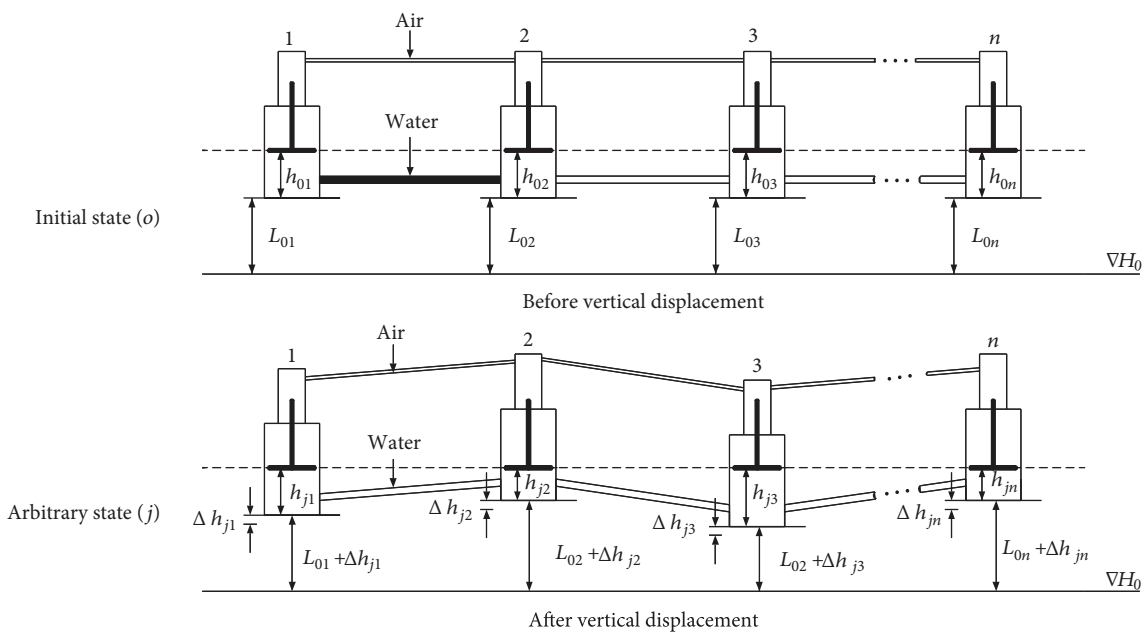

Figure 1: Working principle of a hydrostatic leveling system.

a long-term HLS stability, but a very stable storage ring foundation as well. The high precision of the HLS over short periods even allows the observation of structural distortion induced by the gravitational forces of the sun and the moon (i.e., the tide effect). Morishita and Ikegami [10] applied an HLS composed of 13 sensors to improve the operational stability of the Japan Proton Accelerator Research Complex (J-PARC) linac by providing a monitoring precision of about 0.02 to 1 mm. A periodic tilt induced by the tide effect was measured with this HLS, indicating that the system can provide essential monitoring information for guaranteeing safe J-PARC linac operation. Although HLSs have many advantages, the significant effect of temperature on the specific volume of liquid greatly reduces the stability of such systems [11–14]. Therefore, to obtain the actual deformation of a monitoring target, the measurements should be further processed to reduce the effect of environmental temperature on the monitoring results.

This paper focuses on monitoring the vertical displacement responses of a transmission tower base using the HLS. At the data processing stage, we analyzed the effect of environmental temperature on the measurements and developed four processing schemes to reduce the effect of temperature. The four processing schemes include processing measurements day by day, monthly, quarterly, and annually. The results demonstrate that the quarterly processing scheme provides the most accurate results of the four schemes considered.

2. Working Principle of Hydrostatic Leveling Systems

HLSs employ a highly accurate technique based on the principle of communicating vessels to monitor differential vertical settlements. As shown in Figure 1, the instrument is composed of vessels linked by a double circuit consisting of a liquid circuit and an air circuit.

The HLS shown in Figure 1 is composed of n monitoring points $(1, 2, 3, \ldots, n)$, where monitoring point 1 is denoted as the reference point. In the initial state, the height differences between assembly planes of the vessels and the base height ∇H_0 are $L_{01}, L_{02}, L_{03}, \ldots, L_{0i}, \ldots, L_{0n}$. The distances between water levels and assembly planes are $h_{01}, h_{02}, h_{03}, \ldots, h_{0i}, \ldots, h_{0n}$. Hence,

$$L_{01} + h_{01} = L_{02} + h_{02} = \mathrm{L} = L_{01} + h_{0i} = L = L_{0n} + h_{0n}. \quad (1)$$

After an unequal settlement between monitoring points, the change in the height differences between the vessel assembly planes and the base height ∇H_0 are $\Delta h_{j1}, \Delta h_{j2}, \Delta h_{j3}, \ldots, \Delta h_{ji}, \ldots, \Delta h_{jn}$, where j denotes the discrete monitoring time. The distances between water levels and assembly planes are $h_{j1}, h_{j2}, h_{j3}, \ldots, h_{ji}, \ldots, h_{jn}$. Hence,

$$\begin{aligned}(L_{01} + \Delta h_{j1}) + h_{j1} = (L_{02} + \Delta h_{j2}) + h_{j2} = \mathrm{L} = (L_{0i} + \Delta h_{ji}) \\ + h_{ji} = \mathrm{L} = (L_{0n} + \Delta h_{jn}) + h_{jn}.\end{aligned} \quad (2)$$

For the j – th monitoring state, the relative settlement of monitoring point i and reference point 1 can be calculated as

$$\Delta H_{ji} = \Delta h_{ji} - \Delta h_{j1}. \quad (3)$$

Combining (1), (2), and (3) yields

$$\Delta H_{ji} = (h_{j1} - h_{ji}) - (h_{01} - h_{0i}). \quad (4)$$

Therefore, we can calculate the relative settlement of any linked monitoring point and reference point using the distance measurements between the water levels and the vessel assembly planes (i.e., $h_{j1}, h_{j2}, h_{j3}, \ldots, h_{ji}, \ldots, h_{jn}$) obtained by the sensors.

The main types of HLS sensors include a differential-transformer type, photoelectric type, vibrating-wire type, capacitor type, ultrasonic type, and pressure-difference type. The present study employed the model 4650 Settlement System (Geokon Inc., USA) shown in Figure 2, with its main specifications listed in Table 1 (http://www.geokon.com). The 4650 Settlement System is designed to measure the differential settlement between two points. A reservoir is located at a stable reference point and is connected to a sensor located at the settlement point by two liquid-filled tubes. The sensor senses the pressure of liquid within the tube, and this provides a measure of the height of the liquid column and hence a measure of the elevation difference between the reservoir and the sensor.

Temperature effects on liquid volume and on the expansion and contraction of the liquid confines can be quite complex (i.e., systems exposed to sunlight may suffer from rapid temperature changes at different parts of the system causing significant fluctuation of the readings). According to [15], the temperature can affect the system in two ways. One is due to the difference in the coefficients of thermal expansion of the liquid and its enclosure, the tubes, which causes a change in the apparent volume of liquid in the system. The other one is due to the existence of a thermal gradient across the system, which causes a density gradient in the liquid. Considering these effects, the elevation, H_{T}, corrected for temperature is given by

$$H_{\mathrm{T}} = \mathrm{H}_0 - [(R_1 - R_0)G + (T_1 - T_0)K] - \Delta H_{\mathrm{res}}, \quad (5)$$

where H_0 is the sensor elevation at installation, ΔH_{res} is any change of the fluid level inside the reservoir sight glass, R_1 is the subsequent sensor reading, R_0 is the initial sensor reading, T_0 is the initial temperature, T_1 is the current temperature, G (meters/digit) is the calibration factor supplied with the sensor, and K is the temperature correction factor included on the calibration sheet. It is worth noting that the heterogeneity of temperatures along the line of sensors can also impact the measurement results. Considering that the thermosealed HLS pipes were used and the monitoring system has the ability to control thermosealed properties, the effect should be negligible. Therefore, we only consider here the impacts raised by temperature near the sensors.

Accordingly, the settlement (ΔH_i) between reference point (denoted as ref) and settlement point (denoted as i) is determined as follows:

$$\Delta H_i = [(R_{1i} - R_{0i})G_i + (T_{1i} - T_{0i})K_i] - [(R_{1\mathrm{ref}} - R_{0\mathrm{ref}})G_{\mathrm{ref}} + (T_{1\mathrm{ref}} - T_{0\mathrm{ref}})K_{\mathrm{ref}}]. \quad (6)$$

Figure 2: Geokon model 4650 hydrostatic leveling system.

Table 1: Technical specifications of the Geokon model 4650 hydrostatic leveling system.

Specifications	Value
Standard range	7 m
Sensor accuracy	±0.1% F.S.
Resolution	0.025% F.S.
Temperature range	−20°C to +80°C
Frequency range	2000–3500 Hz

3. Experimental Results and Analysis

3.1. Experimental Background and Program. The settlement of the power transmission tower can cause distortion of the tower body and even lead to the overall inclination and collapse of the tower body. The monitoring target in project is a power transmission tower (denoted as 163# tower) with a height of 74.4 m, which supports a 500 kV power transmission line from Pingshi city to Shaoguan city. The steep hillside where the tower locates experienced a slight landslide and has been reinforced with anchoring technology. To ensure the safety of the tower, a close monitoring is needed. Conventionally precision leveling is the first choice for such a purpose. However, due to that fact the maximum height difference between the four transmission tower footings is about 6 m, it is very difficult to carry out leveling. In order to automatically monitor the stability of the foundation of 163# tower in near real time, we have installed multiple types of sensors (i.e., 7 m range HLS, etc.) on the foundation of 163# tower and collect sensor data based on GPRS wireless network (see Figure 3). The monitoring system consists of a model 4650 HLS including a reference sensor and a monitoring sensor (denoted as S1 and S2, respectively (Figure 2)), a BGK 6150 dual-axis slope sensor (denoted as Q1), and three BGK 3427 displacement meter sensors (denoted as W1, W2, and W3, respectively). Figure 4 illustrates the sensor

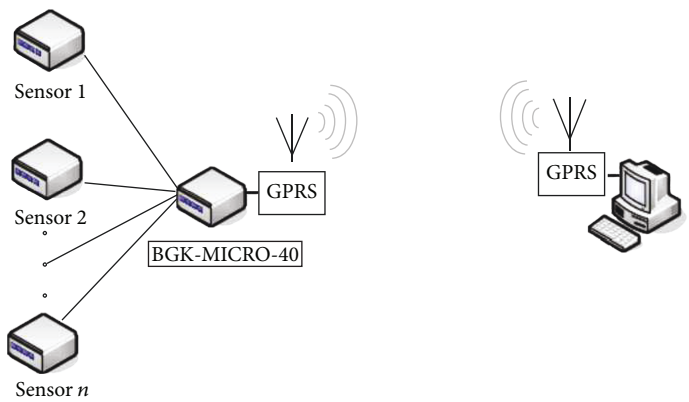

Figure 3: Wireless sensor monitoring network.

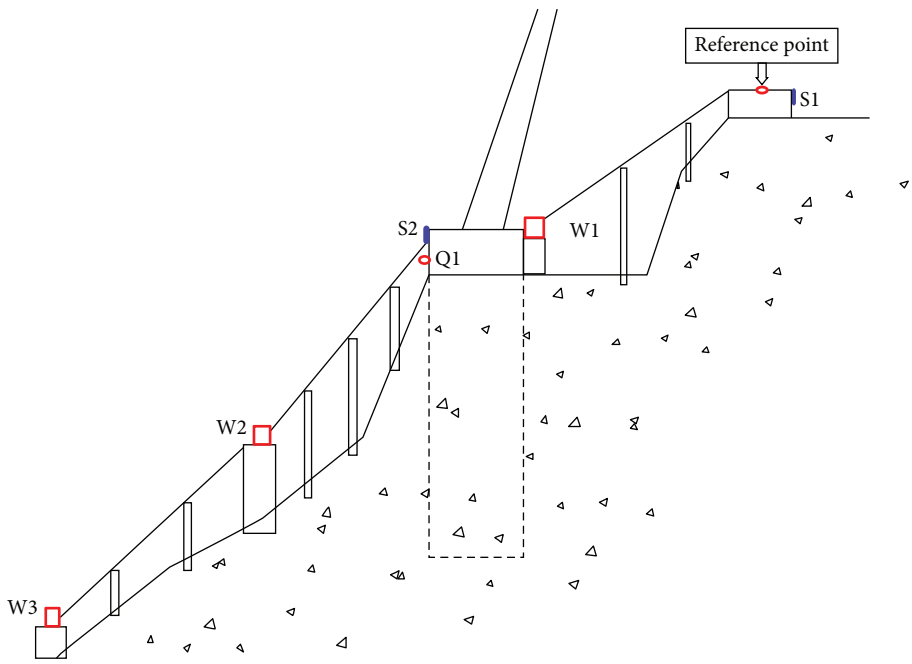

Figure 4: The sensor installation profile along the 163# tower footing.

installation profile along the 163# tower footing, and shown in Figure 5 are the in situ pictures of the monitoring system, and the reference point is made of steel pipe drilled into the rock layer (see Figure 5). All sensors were installed by professional technicians of China Geokon and working properly during the monitoring period. Considering that the systems were calibrated and under normal operation status, there should be no systematic calibration errors in the measurements. The HLS was mainly employed for monitoring the vertical displacement of one of the transmission tower footings, where S1 and S2 were installed on a reference station and monitoring station, respectively. Sensor Q1 (mounted on the top of transmission tower footing) was mainly employed for monitoring the horizontal displacement of the transmission tower footing in two perpendicular directions, expressed as the A and B directions in Figure 5. Sensor W1, W2, and W3 were mainly employed for monitoring displacement in the slope near the top of monitored transmission tower footing; in addition, sensor monitoring results from W1, W2, W3, and Q1 can also be used to check the results of HLS. After sensor installation, continuous monitoring was conducted for 2 years (i.e., January 1, 2014, to December 31, 2015) with a sample rate of 6 h. Sensor data acquisition was accomplished using the Geokon BGK-Micro-40 data acquisition system (http://www.geokon.com.cn/), which automatically recorded and transmitted data at 0 : 00, 6 : 00, 12 : 00, and 18 : 00 hours every day based on the GPRS wireless network.

3.2. Integrated Analysis of Original Experimental Data. Due to power interruption and incorrect setting of the sampling rate, 347 monitoring records for each sensor were missing. Overall, 2573 monitoring data records for each sensor were successfully obtained. Subsequently, 91 monitoring data

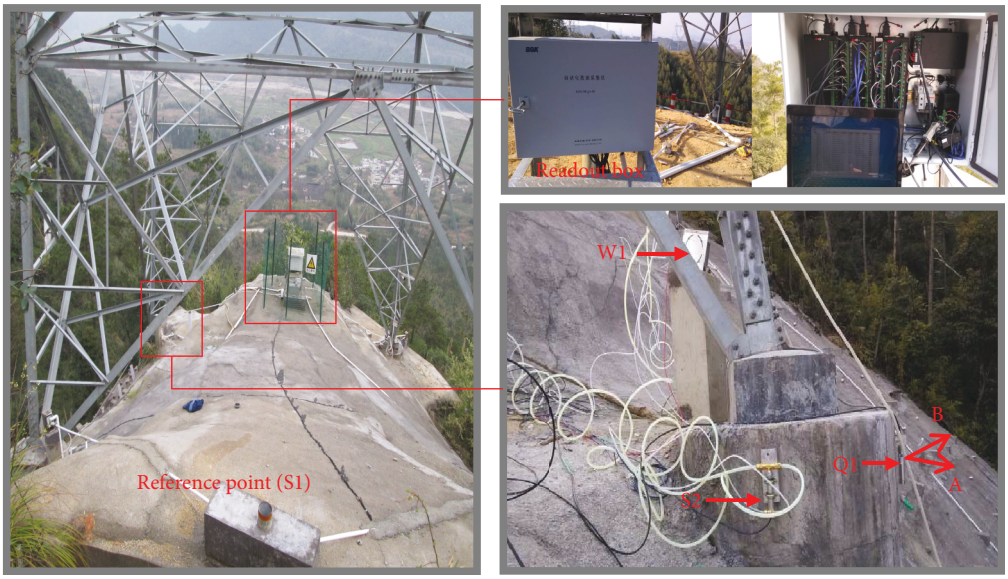

Figure 5: The field map of monitoring system for 163# tower.

Table 2: Statistics of monitoring data.

Sensors	Monitoring data					
	0 : 00	6 : 00	12 : 00	18 : 00	Data eliminated	Elimination rate
S1	590	582	626	684	74 (at 12 : 00); 17 (at 18 : 00)	3.54%
S2	590	582	626	684	74 (at 12 : 00); 17 (at 18 : 00)	3.54%
Q1	590	582	700	701	—	—
W1	590	582	700	701	—	—
W2	590	582	700	701	—	—
W3	590	582	700	701	—	—

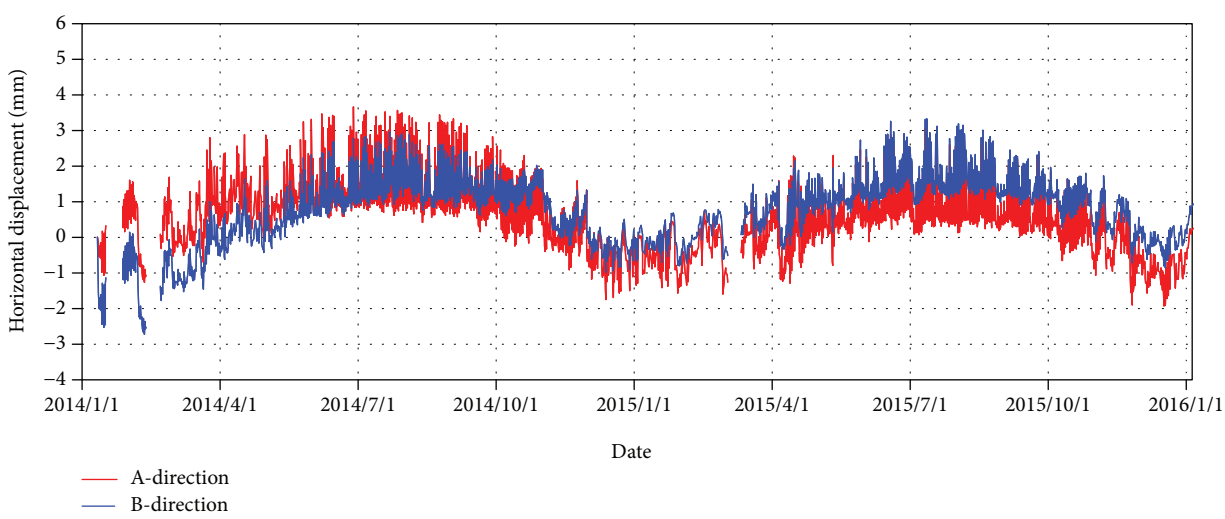

Figure 6: The cumulative displacements of the transmission tower base from Q1.

records of HLS were eliminated on the basis of instrument technical specifications (see Table 1), and the details are listed in Table 2.

The measurement results of Q1 are shown in Figure 6, where the final cumulative displacements of the monitored transmission tower footing were −0.1 mm and 0. 7 mm in the A and B directions, respectively. In addition, the cumulative displacements were within ±3.5 mm in the A and B directions during the monitoring period. The measurement results of W1, W2, and W3 are shown in Figure 7. The

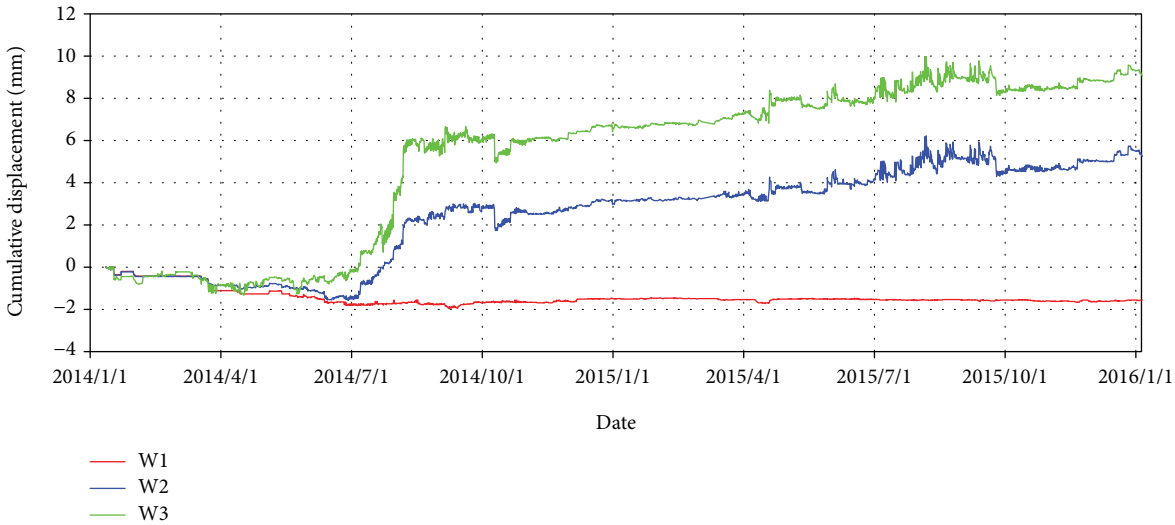

Figure 7: The cumulative displacements of the slope directly above the transmission tower base from W1, W2, and W3.

cumulative horizontal displacements of the slope near the transmission tower footing from W1, W2, and W3 were −1.6 mm, 5.2 mm, and 9.0 mm, respectively. As shown in the figure, the cumulative displacement from W1 gradually tended toward stability; however, the cumulative displacements from W2 and W3 have an accelerated decline process during the period from July to August 2014; the main reason is that there was more rainfall during this time period, after which the displacements gradually becomes slower, and monthly displacement is about 0.2 mm for W2 and W3. Therefore, when considering such factors as the measurement error and weather conditions, the pile foundation of transmission tower footing can be considered as having been stable in the horizontal direction.

The relative settlement of the transmission tower footing was firstly calculated using (6) based on the original measurement data obtained from S1 and S2, and the results are shown in Figure 8. As shown in the figure, the final relative settlement between the reference and monitoring point was −3.8 cm during the monitoring period. In addition, the monitoring results over the full two-year period showed significant annual periodic trends, and the maximum result was −5.4 cm.

The integrated analysis of original experimental data shows that the foundation below the transmission tower footing has a slight displacement (see Figures 6, 7, and 8); however, there is a conflict monitoring result for HLS. Namely, the settlement was notably different in different sampling periods in a day (i.e., the maximum difference of the relative settlement was about 3 cm at 6 : 00 and 12 : 00 on the same day; see Figure 8), and horizontal displacements from sensors W2 and W3 are very small, which is not reasonable even considering the factors such as the temperature effect of the concrete foundation. We attributed the difference to the effect of ambient temperature impact on the HLS which was not well corrected with the calibration parameters provided by the supplier. The reason may be related to the more complex temperature changes in the field environment.

As shown in Figure 9, the vibration frequency and temperature measurements are strongly correlated, particularly for S2, which indicates that the temperature has a significant impact on the sensor readings. The linear correlation for S1 and S2 can also be seen in Figure 10 where the vibration frequency and temperature are presented as two axes, respectively. To reduce the effect, it is required to determine the relationship between vibration frequency and temperature.

As shown in Figure 10, the relationships between vibration frequency and temperature are nearly linear (note that the relationships between temperature and Δh parameter are not linear). Therefore, the relationships can be determined according to a linear model as follows:

$$f = KT + f_0, \tag{7}$$

where f is the frequency measurement, T is the temperature measurement, and f_0 is a constant.

It is important to determine an optimized processing scheme to calculate K for mitigating temperature effect.

Due to the significant effect of temperature on the frequency measurement of vibrating-wire type sensors, and the frequency is the direct observation of HLS, the frequency measurement must be adjusted according to the temperature prior to converting it into a vertical displacement. Including the effect of temperature, variations in the vessel water level of a sensor at any monitoring point or reference point can be calculated as follows:

$$\Delta h = G \times \left(\frac{(f_1 - K \times T_1)^2}{1000 - R_0} \right), \tag{8}$$

where T_1 is the current temperature reading of the sensor and K is the temperature correction coefficient of the frequency measurement. The value of K can be calculated from an appropriate model, which is selected according to the relationship between the temperature and vibration frequency measurements. The appropriate calculation of K represents

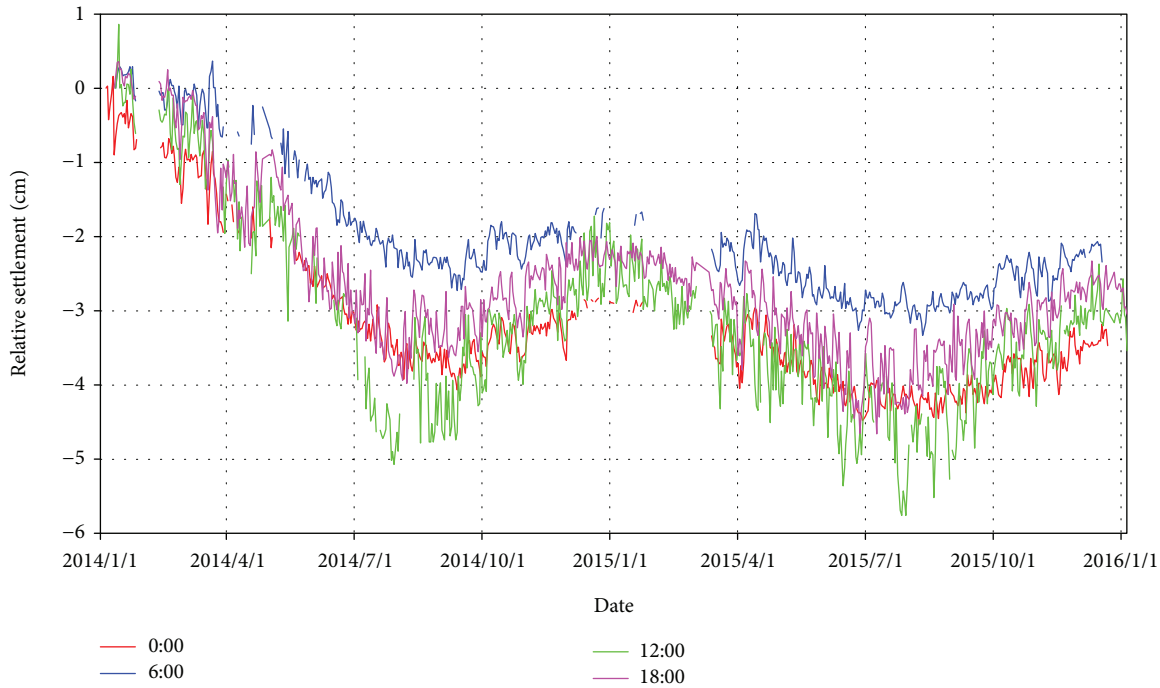

Figure 8: The relative vertical settlement between the reference (S1) and monitoring (S2) points.

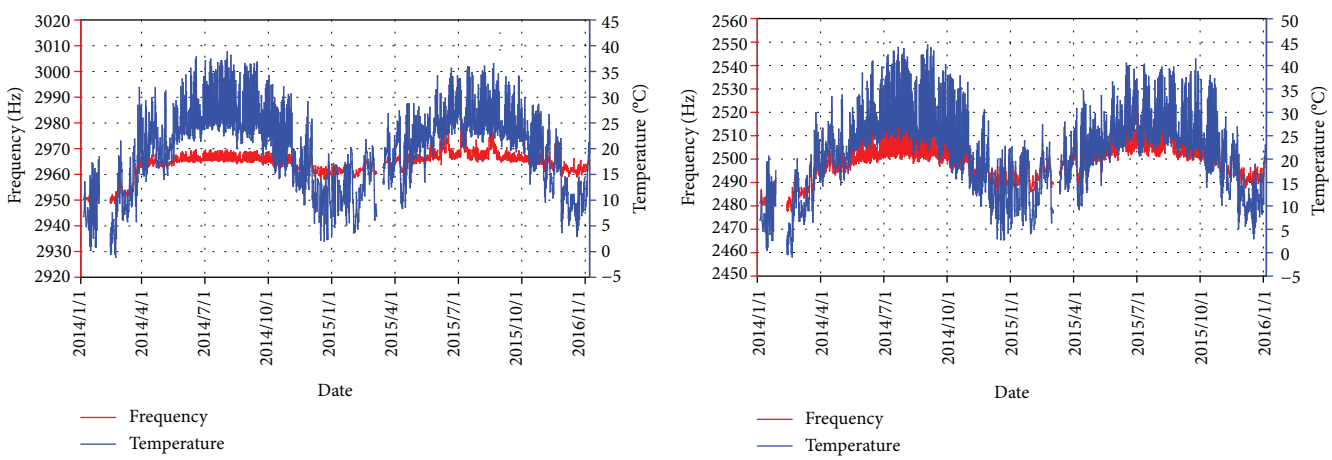

Figure 9: The vibration frequency and temperature measurements of sensors S1 and S2.

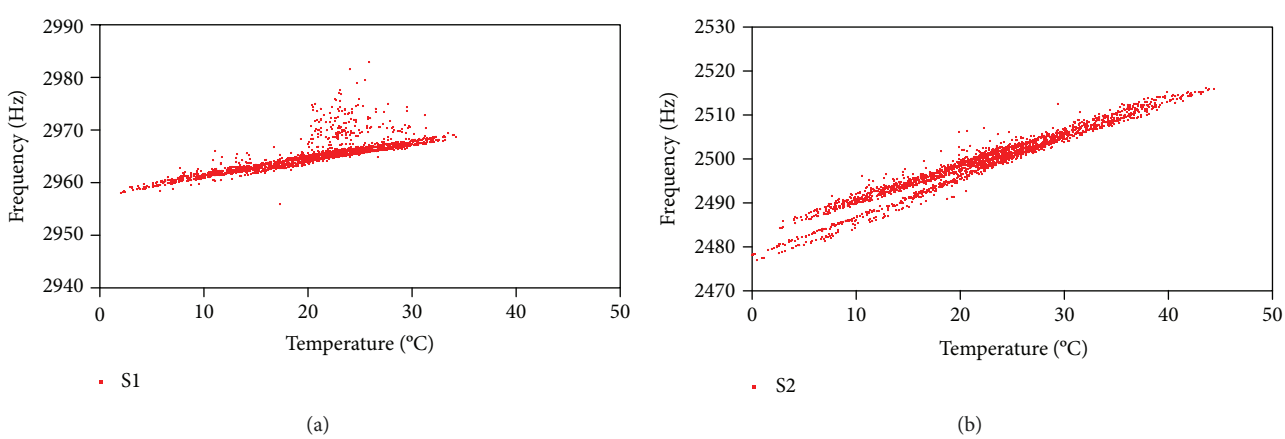

Figure 10: Relationships between vibration frequency and temperature for sensors S1 and S2.

Table 3: Four schemes maximum, minimum, and average values of K, R^2, and RMS for S2.

Schemes	Time	K			R^2			RMS (Hz)		
		Max	Min	Avg	Max	Min	Avg	Max	Min	Avg
A	0 : 00	0.959	0.686	0.914	0.997	0.937	0.972	2.527	0.252	1.424
	6 : 00	0.969	0.749	0.926	0.999	0.920	0.968	2.740	0.119	1.410
	12 : 00	0.926	0.674	0.833	0.996	0.943	0.975	2.923	0.348	1.675
	18 : 00	0.925	0.686	0.869	0.997	0.966	0.983	2.009	0.164	1.212
B	0 : 00	0.860	0.704	0.793	1.000	0.958	0.985	0.388	0.096	0.225
	6 : 00	0.879	0.682	0.803	0.999	0.907	0.980	0.481	0.114	0.209
	12 : 00	0.936	0.632	0.758	0.999	0.933	0.980	0.877	0.175	0.469
	18 : 00	0.886	0.679	0.788	0.999	0.955	0.985	0.501	0.161	0.315
C	0 : 00	0.898	0.698	0.802	0.996	0.953	0.986	0.378	0.172	0.309
	6 : 00	0.908	0.659	0.802	0.998	0.936	0.981	0.697	0.188	0.358
	12 : 00	0.915	0.698	0.767	0.992	0.943	0.980	0.831	0.398	0.608
	18 : 00	0.878	0.747	0.797	0.997	0.973	0.987	0.846	0.282	0.444
D	0 : 00	0.898	0.869	0.884	0.983	0.919	0.951	2.207	1.346	1.777
	6 : 00	0.911	0.901	0.906	0.982	0.898	0.940	2.514	1.260	1.887
	12 : 00	0.840	0.796	0.818	0.989	0.935	0.962	2.756	1.362	2.059
	18 : 00	0.867	0.827	0.847	0.989	0.970	0.979	1.661	1.123	1.392

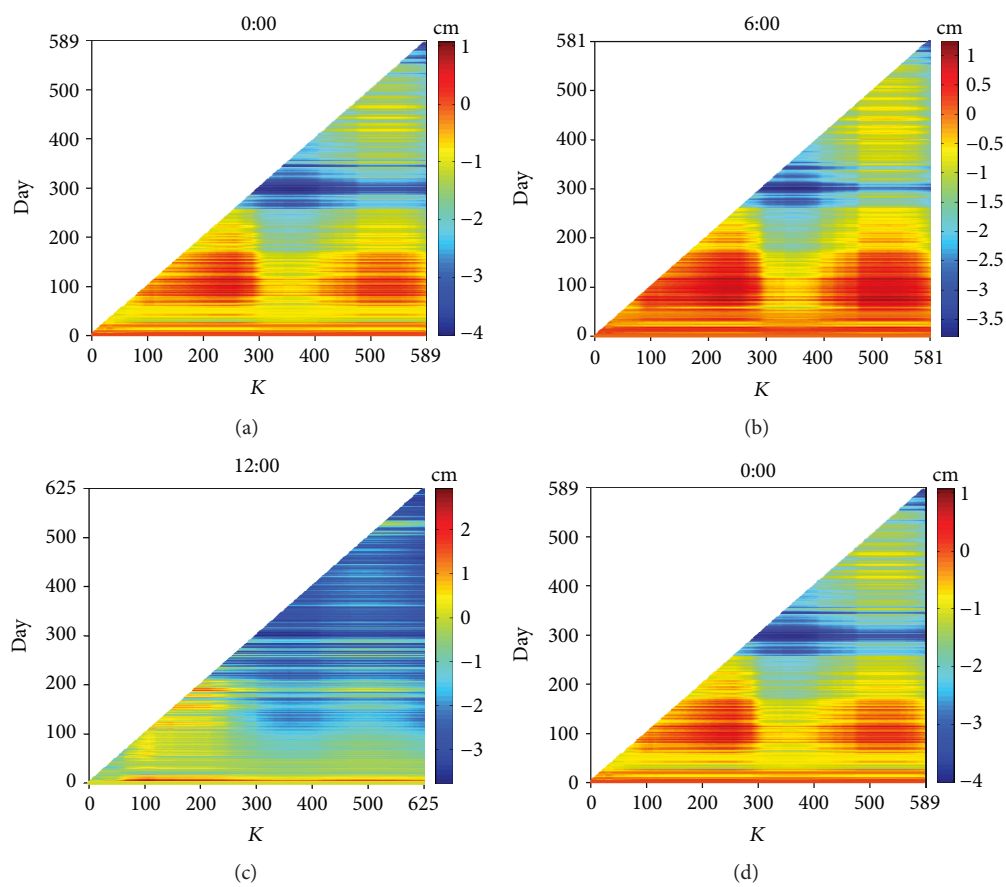

Figure 11: The relative settlements of the monitoring point (sensor S2) at the four daily monitoring periods for each day based on the values of K obtained throughout the process.

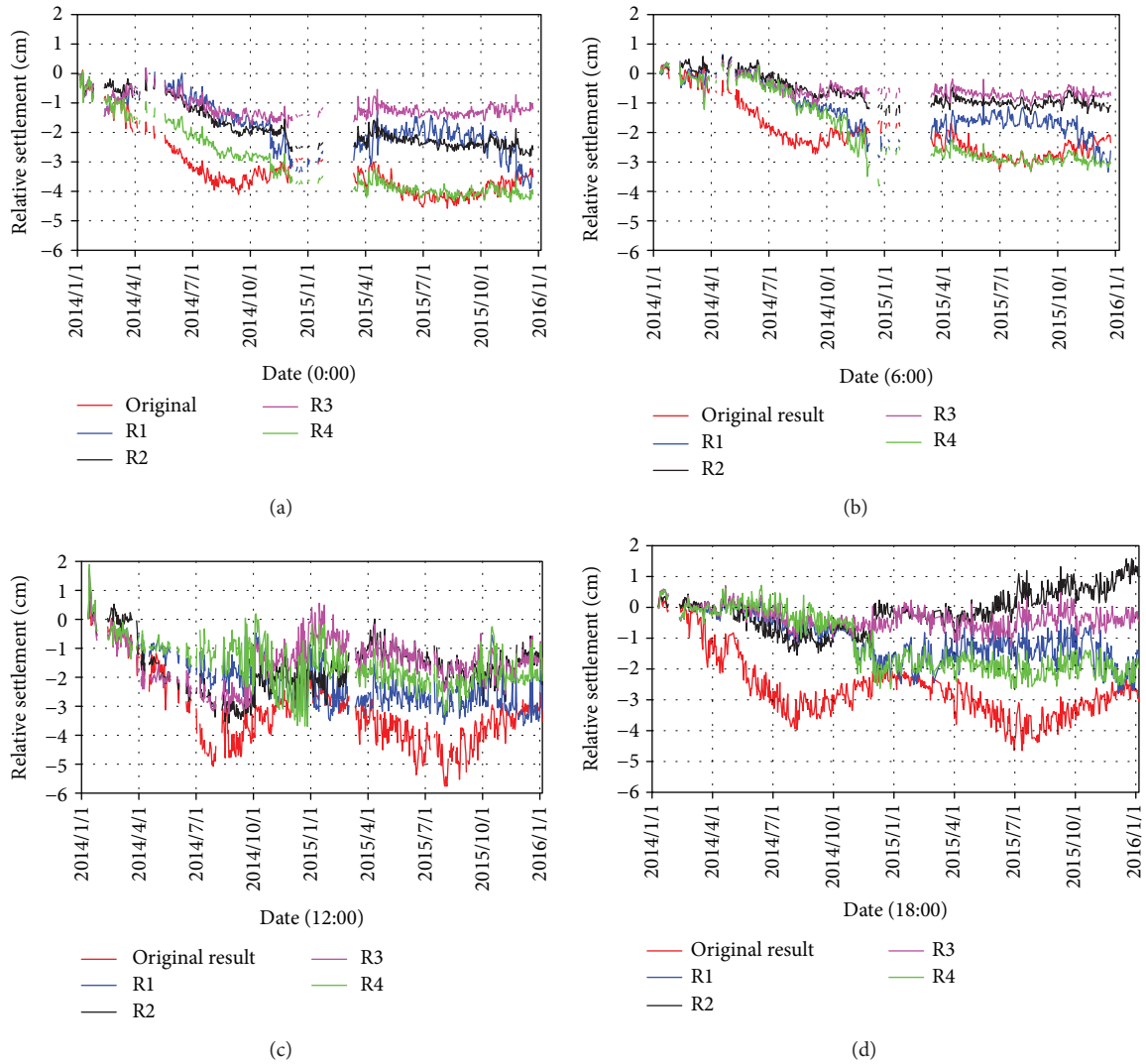

Figure 12: Relative settlements between the reference and monitoring points at the four daily monitoring periods.

one of the primary concerns of this work. Finally, ΔH_i is determined as follows:

$$\Delta H_i = G_i \times \left(\frac{(R_{1i} - K_i \times T_{1i})^2}{1000 - R_{0i}} \right) - G_{\text{ref}} \times \left(\frac{(R_{1\text{ref}} - K_{\text{ref}} \times T_{1\text{ref}})^2}{1000 - R_{0\text{ref}}} \right). \quad (9)$$

3.3. Calculation Schemes for Temperature Correction Coefficient K. In order to minimize the effect of temperature on the vibration frequency observation, the key point is to establish the relationship between temperature and vibration frequency observation of HLS. In Section 3.2, we have analyzed the relationship between vibration frequency and temperature measurements of HLS and the relationships can be determined according to a linear model. The temperature changes have a certain relationship with a specific time period such as days and months. Therefore, the main purpose of calculating K with the day-by-day, monthly, quarterly, and annual monitoring data is to determine the optimal calculation schemes of coefficient K, which is reasonable (see Figure 9). We experiment here to calculate K with the day-by-day, monthly, quarterly, and annual monitoring data, which are denoted as schemes A, B, C, and D, respectively. The main steps are as follows: the coefficient K was firstly computed with selected period monitoring data (for instance, in the quarterly, there are 4 coefficients in one year), and then the selected period raw frequency observation was corrected with the corresponding coefficient K. The final relative settlement between S1 and S2 was calculated with the corrected frequency observation based on (9). All the calculation schemes are applied to both S1 and S2. However, only S2 is taken as an example for discussion and analysis.

The statistics for time sequences of K, the correlation coefficient R^2, and the residual-based root mean square (RMS) obtained according to four calculation schemes are listed in Table 3. It is clear that the average linear

correlation between the vibration frequency and temperature is high because the time sequence values of R^2 are all greater than 0.940. It is also found that the average RMS values of the residuals are less than 0.610 Hz for schemes B and C, indicating that these two processing schemes might be the best.

For further analysis, the relative settlement of S2 was then calculated using (9) at the four daily monitoring periods for each day based on the values of K obtained day by day. The results are shown in Figure 11 for S2, and the horizontal axis represents the number of coefficient K, and the vertical axis represents the number of monitoring days in Figure 11. For example, when the monitoring period is 10 days, Figure 11 shows all calculated K values within 10 days and their corresponding corrected monitoring results (note that the coefficient K is a parameter that is being updated over time). As shown in Figure 11, the relative settlements calculated by the different daily values of K can provide different settlement values for the same day. The results of this data processing scheme become gradually worse with increased monitoring data, which means that the optimal coefficient K may correspond to a certain monitoring time window such as one month.

3.4. Corrected Relative Settlements. The frequency measurements of S1 and S2 were corrected using the values of K obtained by the four calculation schemes discussed, respectively. The variations in the water levels of S1 and S2 were then calculated using (8), and the relative settlement of S2 was calculated by (9). Since it is very meaningful to consider the relative settlement between sensors S1 and S2 rather than an absolute settlement for each sensor, the time sequences of the relative settlements are shown in Figure 12, and the statistics listed in Table 4. In Figure 12 and Table 4, R1, R2, R3, and R4 correspond to the results obtained using calculation schemes A, B, C, and D, respectively. The original result represents the uncorrected result.

As shown in Figure 12 and Table 4, compared with original results, the R3 results are observed to be the best of the four calculation schemes, which provides final relative settlements of −1.1, −0.7, −1.9, and −0.5 cm at 0 : 00, 6 : 00, 12 : 00, and 18 : 00, respectively. Meanwhile, variations in the relative settlements are more stable at 0 : 00, 6 : 00, and 18 : 00. According to calculation scheme C (the quarterly scheme), the relative settlements of S2 from all measurement data were then calculated by (7), (8), and (9), and the results are shown in Figure 13 (the frequency observations of sensors S1 and S2 are independently temperature-corrected). The relative settlements are shown in Figure 14 at 0 : 00, 6 : 00, 12 : 00, and 18 : 00, respectively.

As shown in Figures 13 and 14, the final relative settlements of the monitoring point are −3.8 cm and −1.5 cm before and after temperature correction. During the monitoring period, the maximum relative settlements of the monitoring point are −5.4 cm and −2.7 cm before and after temperature correction. Clearly, the corrected results are consistent with the monitoring results of Q1, W1, W2, and W3 (see Figures 6, 7, and 8), and the settlement results at different times have better consistency (see Figures 8 and 14), indicating that the quarterly processing scheme provides an excellent temperature correction and might be considered for similar monitoring scenarios in future. Based on the above results, we think our temperature corrections results are reliable.

Table 4: Maximum, minimum, and final relative settlement values between the reference and monitoring points (cm) obtained by day-by-day (R1), monthly (R2), quarterly (R3), and annual (R4) processing schemes.

	Time			
	0 : 00	6 : 00	12 : 00	18 : 00
Original result				
Max	0.2	0.4	0.9	0.4
Min	−4.5	−3.3	−5.8	−4.7
Final	−3.5	−2.3	−3.5	−3.0
R1				
Max	0.2	0.6	1.7	0.6
Min	−3.9	−3.3	−3.7	−2.8
Final	−3.2	−2.6	−3.1	−1.6
R2				
Max	0.1	0.6	1.7	1.6
Min	−2.8	−1.4	−3.6	−1.6
Final	−2.5	−1.1	−2.3	1.0
R3				
Max	0.2	0.5	1.4	0.7
Min	−1.8	−1.1	−3.4	−1.3
Final	−1.1	−0.7	−1.9	−0.5
R4				
Max	0.1	0.4	1.9	0.7
Min	−4.3	−3.8	−3.7	−2.7
Final	−4.1	−3.1	−2.1	−2.0

4. Conclusions

This paper focused on methods for refining the measurements obtained from a vibrating-wire HLS by accurately accounting for the temperature effect using four different calculation schemes. Based on the monitoring results obtained for a transmission tower footing, the following conclusions can be drawn.

(1) The integrated analysis of original experimental data demonstrates that the effect of temperature on the HLS exposed to the sun is very large and it is compulsory to consider the temperature correction. In order to reduce the effect of temperature on the HLS, we determined the relationships between vibration frequency and temperature which follows a linear model.

(2) The experimental results demonstrate that the day-by-day, monthly, quarterly, and annually calculation

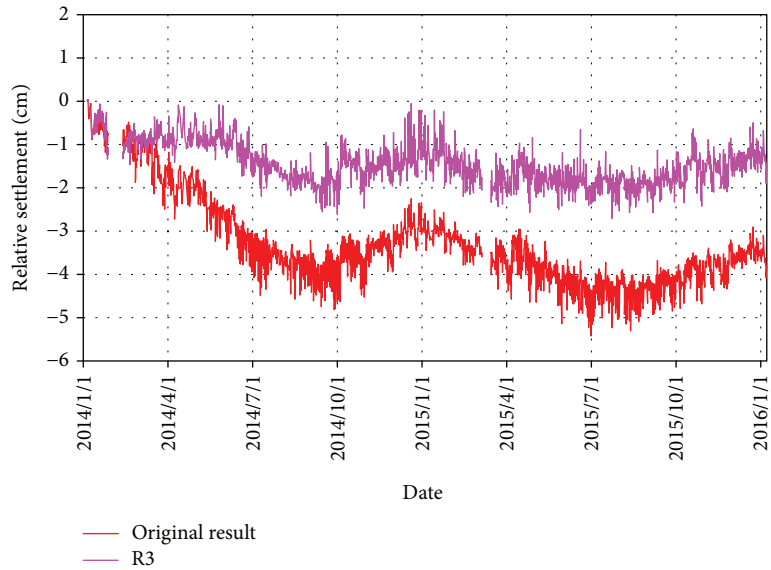

Figure 13: The relative settlements of the monitoring point (sensor S2) obtained by the quarterly scheme.

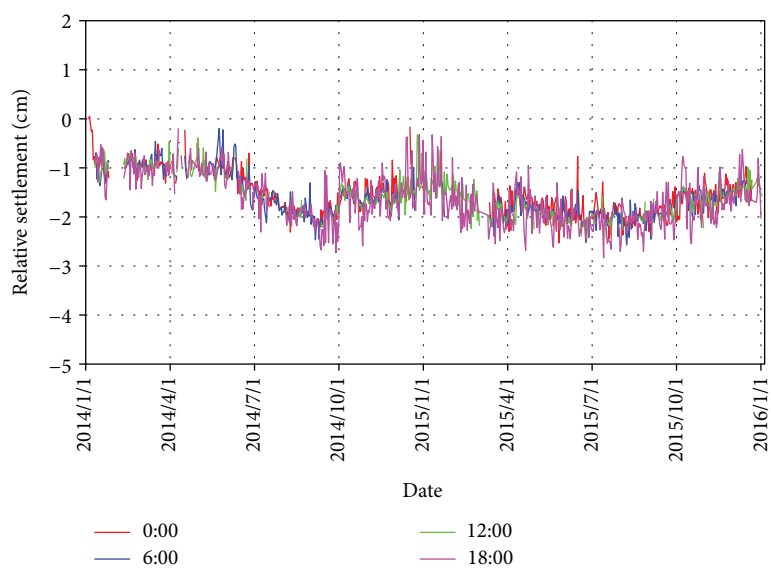

Figure 14: The relative settlements of the monitoring point (sensor S2) obtained by the quarterly scheme at 0 : 00, 6 : 00, 12 : 00, and 18 : 00, respectively.

schemes provide different temperature correction results, while variations in the relative settlements are more reasonable at 0 : 00, 6 : 00, and 18 : 00 from the quarterly calculation scheme. Also, the corrected results are best consistent with the independent monitoring results obtained from a dual-axis slope sensor (Q1) and displacement meters (W1, W2, and W3).

(3) The integrated analysis of experimental results demonstrates that the pile foundation of transmission tower footing has settled, where there is no inclination. Overall, the pile foundation of transmission tower footing is gradually stable.

Data Availability

The data used to support the findings of this study are available from the corresponding author upon request.

Conflicts of Interest

The authors declare that they have no conflicts of interest.

Acknowledgments

The authors gratefully acknowledge the financial support from the National Natural Science Foundation of China (Grant Nos. 41674006, 41774023, and 41304011). They

would also like to thank the anonymous reviewers whose comments improved the clarity of the manuscript significantly.

References

[1] D. Martin, "Deformation movements observed at the European Synchrotron Radiation Facility," in *Proceedings of The 22nd Advanced ICFA Beam Dynamics Workshop on Ground Motion in Future Accelerators*, Stanford, USA, 2000.

[2] J. Figueiras, C. Félix, and B. Afonso Costa, "Testing and monitoring of a centenary arch bridge," *Structure and Infrastructure Engineering*, vol. 1, no. 1, pp. 63–73, 2005.

[3] Y. Robert-Nicoud, B. Raphael, O. Burdet, and I. F. C. Smith, "Model identification of bridges using measurement data," *Computer-Aided Civil and Infrastructure Engineering*, vol. 20, no. 2, pp. 118–131, 2005.

[4] O. Burdet, "Experience in the long-term monitoring of bridges," in *3rd fib International Congress (No. EPFL-CONF-163103)*, pp. 108–113, 3rd fib International Congress, Washington DC, USA, 2010.

[5] C. Rodrigues, C. Félix, A. Lage, and J. Figueiras, "Development of a long-term monitoring system based on FBG sensors applied to concrete bridges," *Engineering Structures*, vol. 32, no. 8, pp. 1993–2002, 2010.

[6] Z. J. Chen, N. N. Zhang, and X. W. Zhang, "Settlement monitoring system of pile-group foundation," *Journal of Central South University of Technology*, vol. 18, no. 6, pp. 2122–2130, 2011.

[7] Z. Z. Yin, "Application of hydrostatic leveling system in metro monitoring for construction deep excavation above shield tunnel," *Applied Mechanics and Materials*, vol. 333-335, pp. 1509–1513, 2013.

[8] D. Martin, "The European Synchrotron Radiation Facility Hydrostatic Levelling System–twelve years experience with a large scale hydrostatic levelling system," *Proceedings of the 7th International Workshop on Accelerator Alignment*, Spring-8, 2002.

[9] F. Q. Wei, L. Rivkin, and A. Wrulich, "Experiences with the Hydrostatic Leveling System at the SLS," in *Proceedings of EPAC*, p. 1651, Lucerne, Switzerland, 2000.

[10] T. Morishita and M. Ikegami, "The slow-ground-motion monitoring based on the hydrostatic leveling system in J-PARC linac," *Nuclear Instruments and Methods in Physics Research Section A: Accelerators, Spectrometers, Detectors and Associated Equipment*, vol. 602, no. 2, pp. 364–371, 2009.

[11] M. Schlösser and A. Herty, "High precision survey and alignment of large linear colliders–vertical alignment," *Proceedings of the Seventh International Workshop on Accelerator Alignment*, Spring 8, Japan, 2002.

[12] C. Zhang, K. Fukami, and S. Matsui, "From the HLS measurement for ground movement at the SPring-8," *Stainless Steel (SUS)*, vol. 4, pp. X10–X15, 2004.

[13] L. Schueremans, K. Van Balen, P. Smars, V. Peeters, and D. Van Gemert, *Hydrostatic Levelling System–Monitoring of Historical Structures*, Structural Analysis of Historical Constructions, New Delhi, 2006.

[14] E. Meier, A. Geiger, H. Ingensand et al., "Hydrostatic levelling systems: measuring at the system limits," *Journal of Applied Geodesy*, vol. 4, no. 2, pp. 91–102, 2010.

[15] P. F. Pellissier, "Hydrostatic leveling systems," *IEEE Transactions on Nuclear Science*, vol. 12, no. 3, pp. 19-20, 1965.